

**CONSTRAINTS ON THE PARENTAL MELTS OF ENRICHED SHERGOTTITES FROM IMAGE ANALYSIS AND HIGH PRESSURE EXPERIMENTS** M. Collinet<sup>1,2</sup>, E. Médard<sup>2</sup>, B. Devouard<sup>2</sup> and A. Peslier<sup>3</sup>, <sup>1</sup>Département de Géologie, Université de Liège, Liège 4000, Belgium, [mcollinet@doct.ulg.ac.be](mailto:mcollinet@doct.ulg.ac.be), <sup>2</sup>Laboratoire Magmas et Volcans, Université Blaise Pascal – CNRS – IRD, Clermont-Ferrand F-63038, France, <sup>3</sup>Astromaterials Research and Exploration Science, NASA-Johnson Space Center, Houston, TX 77058, USA

**Introduction:** Martian basalts can be classified in at least two geochemically different families: enriched and depleted shergottites. Enriched shergottites are characterized by higher incompatible element concentrations and initial  $^{87}\text{Sr}/^{86}\text{Sr}$  and lower initial  $^{143}\text{Nd}/^{144}\text{Nd}$  and  $^{176}\text{Hf}/^{177}\text{Hf}$  than depleted shergottites [e.g. 1, 2]. It is now generally admitted that shergottites result from the melting of at least two distinct mantle reservoirs [e.g. 2, 3]. Some of the olivine-phyric shergottites (either depleted or enriched), the most magnesian Martian basalts, could represent primitive melts, which are of considerable interest to constrain mantle sources. Two depleted olivine-phyric shergottites, Yamato (Y) 980459 and Northwest Africa (NWA) 5789, are in equilibrium with their most magnesian olivine (Fig. 1) and their bulk rock compositions are inferred to represent primitive melts [4, 5]. Larkman Nunatak (LAR) 06319 [3, 6, 7] and NWA 1068 [8], the most magnesian enriched basalts, have bulk Mg# that are too high to be in equilibrium with their olivine megacryst cores. Parental melt compositions have been estimated by subtracting the most magnesian olivine from the bulk rock composition, assuming that olivine megacrysts have partially accumulated [3, 9].

However, because this technique does not account for the actual petrography of these meteorites, we used image analysis to study these rocks history, reconstruct their parent magma and understand the nature of olivine megacrysts.

Our image analysis results are supported by a series of high-pressure experiments performed on LAR 06319 bulk rock composition to test if it could represent a primitive melt, and understand its crystallization history.

**Methodology:** Element maps (Si, Ti, Al, Cr, Fe, Mn, Mg, Ca and Na) were acquired with a Cameca SX100 electron microprobe on thin-sections of LAR 06319 and NWA 1068. Classified images in which pixels of similar composition are grouped into homogeneous classes were created using the MultiSpec and ImageJ softwares. Pixels counts from each class provides a modal composition that can be transformed into a bulk rock composition if composition and density of mineral phases are known. Phase composition for each class were determined either with microprobe point analysis or by averaging pixels from quantified element maps. Mg# maps and major element profiles of megacrysts were also created from quantified maps.

On classified images, olivine crystals were separated into four compositional classes. Classes were progressively subtracted from the modal composition (starting with the class corresponding to megacryst cores) to eliminate the effect of crystal accumulation (Fig. 1).

High-pressure experiments were carried out on a synthetic bulk LAR 06319 composition [6] with a piston cylinder apparatus using Pt-Graphite double capsules.

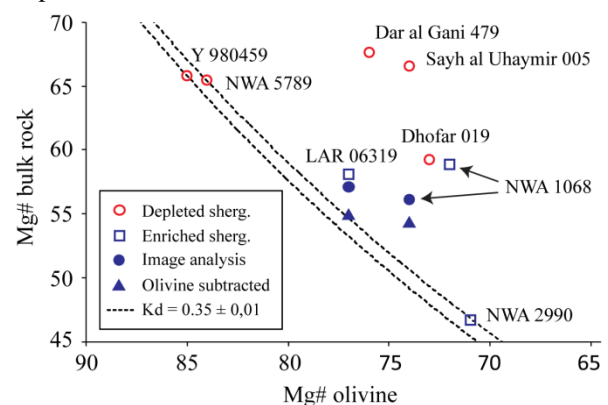


**Fig. 1.** Comparison of bulk rocks and olivine megacryst Mg#. Data from [9] and references inside.

**Results and discussion:** Our bulk rock compositions are identical within error to those determined by classical destructive methods [6, 8]. Image analysis can thus provide accurate chemical compositions representative of the bulk rocks. In NWA 1068, terrestrial carbonate that could not be cleaned before destructive analysis [8] can be isolated and excluded by image analysis. Our recalculated NWA 1068 bulk rock composition (free from terrestrial carbonate) has a  $\text{CaO}/\text{Al}_2\text{O}_3$  ratio of 1.1 identical to the one of LAR 06319 [6] that contrast with destructive analysis results ( $\text{CaO}/\text{Al}_2\text{O}_3 = 1.4$  [8]). This indicates a relatively homogeneous supra-chondritic ratio of  $\sim 1.1$  for parental magmas of enriched shergottites (compared to  $\sim 1.2$  for depleted shergottites [5]).

To reach a melt composition in equilibrium ( $\text{Mg}\# = 54.6$ ) with the most magnesian olivine ( $\text{Fo}_{77}$ ) from LAR 06319 composition, the whole megacryst olivine has to be subtracted (Fig. 1). However, the most magnesian remaining olivine is  $\text{Fo}_{61}$  instead of  $\text{Fo}_{77}$ , indicating that simple accumulation is not a viable process. For NWA 1068, subtraction of megacrysts is not even sufficient to reach the equilibrium ( $\text{Mg}\# = 50.6$ ) with

the most magnesian olivine ( $\text{Fo}_{74}$ ). Hence, it clearly appears that olivine accumulation cannot account alone for the observed disequilibrium. The high Mg# of LAR 06319 and NWA 1068 bulk rocks also result from the high pyroxene Mg#. Previous calculations [3, 9] overestimated significantly the quantity of accumulated Mg-rich olivine present in these rocks, and thus proposed parental melts are probably inaccurate.

Furthermore, megacryst cores of olivine-phyric shergottites are only slightly zoned (Fig. 2). This observation is also not consistent with simple Rayleigh fractional crystallization. Some Fe-Mg re-equilibration has to be considered, indicating that the most Mg-rich olivine does not necessarily represent the first crystallized olivine.



**Fig. 2.** Forsterite content profiles in megacrysts of olivine-phyric shergottites Y 980459 [10], NWA 5789 [5], LAR 06319 and NWA 1068 (from Mg# maps).

Analysis of trace elements in megacrysts melt inclusions [6, 11] make a xenocrystic origin unlikely. These results, together with a crystal size distribution analysis [6] suggest that megacrysts cores crystallized slowly and continuously re-equilibrate with the melt, probably in a magma conduit or chamber, while megacrysts rims and groundmass olivine crystallized faster during the eruption. Olivine accumulation cannot be completely ruled out but our results suggest that megacrysts re-equilibration is the dominant process responsible for the observed disequilibrium. LAR 06319 and NWA 1068 parental melts are probably close to the bulk rock compositions.

As already discussed, liquidus olivine in experimental run products is slightly more magnesian ( $\text{Fo}_{80}$  at 0.5 GPa) than megacryst cores in LAR 06319 ( $\text{Fo}_{77}$ ). The first pyroxene to crystallize is an orthopyroxene with a low CaO content varying from 1 to 1.5 wt %. A preliminary phase diagram is presented in Fig. 3. The bulk composition is multiply saturated with olivine and orthopyroxene, which represent likely residual mantle minerals at  $1.0 \pm 0.2$  GPa and  $1445 \pm 20$  °C. A magma of LAR 06319 composition could have last equilibrated with the Martian mantle under those conditions. It is interesting that ol-opx multiple saturation points were reported at similar pressures for magma composi-

tions of Y 980459 [4] and Gusev basalts [12] inferred to represent primitive melts. LAR 06319 composition could also be close to a primitive melt equilibrated at a depth of 80 to 100 km in the Martian mantle.

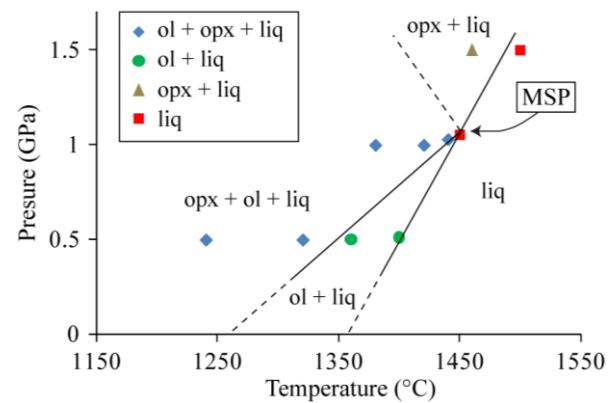


**Fig. 3.** Preliminary experimental P-T phase diagram. MSP: ol-opx multiple saturation point.

**References:** [1] Shih C. -Y. et al. (2005) *Ant. Meteor. Res.*, 18, 46-65. [2] Shafer J. T. et al. (2010) *Geochim. Cosmochim. Ac.*, 74, 7307-7328. [3] Basu Sarbadhikari A. et al. (2011) *Geochim. Cosmochim. Ac.*, 75, 6803-6820. [4] Musselwhite D. S. et al. (2006) *Meteorit. Planet. Sci.*, 41, 1271-1290. [5] Gross J. et al. (2011) *Meteorit. Planet. Sci.*, 46, 116-133. [6] Basu Sarbadhikari A. et al. (2009) *Geochim. Cosmochim. Ac.*, 73, 2190-2214. [7] Peslier et al. (2010) *Geochim. Cosmochim. Ac.*, 74, 4543-4576. [8] Barrat J. A. et al. (2002) *Geochim. Cosmochim. Ac.*, 66, 3505-3518. [9] Filiberto J. and Dasgupta R. (2011) *EPSL*, 304, 527-537. [10] Usui T. et al. (2008) *Geochim. Cosmochim. Ac.*, 72, 1711-1730. [11] Shearer C.K. et al. (2008) *Meteorit. Planet. Sci.*, 43, 1241-1258. [12] Monders A.G. et al. (2007) *Meteorit. Planet. Sci.*, 42, 131-148.